JOURNAL OF BASIC SCIENCE AND ENGINEERING

Study on optimization of coating parameters on Adhesive strength, wear rate of nano coatings

ShiddalingayyaMathad[1*], Raghavendra C R[2], Shivakumar G[3], Mallikarjuna K[4], Jhansilakshmi K P[5]

[1]Department of Mechanical Engineering, Government Polytechnic, Hanagal, Karnataka, India
[1]Research Scholar, Department of Mechanical Engineering, Government Engineering College, Haveri,Karnataka, India
[2,5]Department of Mechanical Engineering, Government Engineering College, Haveri, Karnataka, India
[3]Department of Mechanical Engineering, Government Polytechnic, Immadihalli, Bangaluru. Karnataka, India
[4]Department of Mechanical Engineering, Government Polytechnic, Bellary, Karnataka, India

DOI: https://doie.org/10.1223/Jbse.2024824173

Abstract
The present work is concentrated on the electro co-deposition of Ni particles with nano Al2O3 nano particles as secondary phase particles. The coating is carried out by considering bath temperature, current density and nano particle insertion in the bath are considered for optimization of coating parameters. The design of experiments are planned as per the response surface methodology technique by central composite design method. The adhesive strength of the coating with Al6061 substrate material is carried out by scratch test. The traction force obtained during the scratch test is considered as the adhesive strength of the coating. The wear rate is carried out on pin-on-disc test rig. The temperature and current density these parameters has a good combination of adhesive strength for constant load value 32.33N and traction force value is 61N. The coating replicates the profile of the substrate very closely. Traction force is influenced by the hardness of the material. The interaction effect of particle loading with current density is more influencing on wear resistance. The optimized values are temperature of 30^{o}C, current density of 1 A/dm^2 and particle loading of 4.8 g/L.

Key words: Nano coating, Wear rate, Scratch test, Electro co-deposition, Ni-Al_2O_3 nano coatings, Taguchi, Optimization.

1. Introduction

A coating is a layer that is mainly applied to the surface of an object; it is generally referred to the substrate. The motivation of applying the coating may be beautiful, useful, or both [1,2]. Coating technology is fundamentally dependent upon good adhesion between the coating and the substrate, and in many cases adhesion is the limiting factor for the wider application of the technology [3]. A composite coating is the combination of two or more substances that offer protection against corrosion. The primary use of electrodeposited composites is in wear resistance, lubrication and corrosion resistance. The metals are scattering solidified by the incorporation of oxide particles like SiC, Al_2O_3 and TiO_2 or fibers many more [4–9]. Adhesive strength refers to the ability of an adhesive to stick to a surface and bond two surfaces together. It is measured by assessing the maximum tensile stress needed to detach or unstick the adhesive perpendicular to the substrate. Determination of the failure point can be critical for the last utilization of the material and the adhesive. There are a large number of different adhesive products, which require different testing methods to characterize the properties of the material.

Electro deposition is a method of co-depositing of micron or nano sized particles of metallic or non-metallic compounds and polymers with a metal or alloy matrix. During the last decades, the main work carried out in this field is aimed almost entirely to the production of wear- and corrosion-resistant coatings, self-lubricating systems and dispersion- strengthened coatings [10–13].

Narasimman et al. [14] investigated Nickel-nano and micro silicon carbide composites were electrodeposited on steel substrate sediment co-deposition technique was used in conventional watts bath with tetra methyl ammonium hydroxide as the surfactant. Deposited with varying volume% by varying SiC in bath and operating conditions. Resistance of the composites wear and scratch and their surface roughness ere measured and compared. It is conformed that, given volume of the of the particles in the deposit. Ni-Sic nano composites exhibit much lower wear loss and higher scratch resistance compared to Ni-SiC micro composites. Vaezi et al. [15] used Ni-SiC nano composite coatings with different contents of SiC nano particulates. Deposition varies with SiC concentration in bath, current density, stir rate, and temperature of plating bath. Modified watts bath and copper substrate was used in accordance with Zimmerman et al. By varying the current density from 20 – 70 mA/cm2 At 30 °C, deposition Ni-SiC is 70%At 60 °C, deposition increases from 73 to 84%. The crystalline size of Nickel deposit is 28 nm and with deposition of SiC it led to reduction up to 11 nm. Incorporation of SiC in nano crystalline matrix has also resulted in increase in hardness from 260 to 450 VHN. Narasimman et al. [16] found that for a given volume % of the particles in the deposit, Ni–SiC, nano composites exhibit much lower wear loss and higher scratch resistance compared to Ni–SiC micro composites.

Sathish et al. [17] fabricated WC-12wt%Co and Yttria-stabilized Zirconia coatings using Atmospheric Plasma Spraying technique. The Microstructural Characterization of the coatings was carried out using Scanning electron microscope(SEM). Potentiostat was employed to perform corrosion testing for the bare substrate and the coatings in 5 wt %Nacl solution.

Chang et al. [18] used Ni–Co/nano-Al2O3 (Ni–Co/Al2O3) composite coatings which were prepared under pulse reversal current (PRC) and direct current (dc) methods respectively. The microstructure of coatings was characterized by means of XRD, SEM and TEM. Both the Ni–Co alloy and composite coatings exhibit single phase of Ni matrix with face-centered cubic (fcc) crystal structure, and the crystal orientation of the Ni–Co/Al2O3 composite coating was transformed from crystal face (2 0 0) to (1 1 1) compared with alloy coatings. The hardness, anti-wear property and macro-residual stress were also investigated. Gadhari et al. [19] investigate the electroless Ni–P–Al2O3 composite coatings have found wide range of applications due to their high hardness and wear resistance. The present study the influence of coating process parameters on the microhardness of electroless Ni–P–Al2O3composite coating with the help of Taguchi analysis. Four parameters, namely, concentration of nickel sulphate as a nickel source, concentration of sodium hypophosphite as a reducing agent, concentration of Al2O3 particles as concentration of second phase particles, and annealing temperature, are considered and fitted into an L27 orthogonal array to find out the optimized condition for improved hardness of the coating. Fayomi et al. [20] studied on the microstructure, and mechanical performance of Zn-Al2O3-SiC film co-deposited on mild steel substrate were delivered by electrodeposition technique. Yue-hai et al. [21] investigate the properties and structure of electrodeposited RE (CeO2)-Ni-W-P-SiC composite coating were investigated. The results show that the hardness and electrodepositing speed of composite coatings obtained at an impulse current are higher than those at a direct current. The hardness and wear resistance of the coating are obviously increased by adding RE and SiC. The hardness of the coating increases with the increase of treatment temperature and current density, and reaches the optimum value at 400 and at 10 ℃ A/dm2, respectively. The optimum operation parameters of electrodeposition of the composite coating are as follows: pH value is 4.5, bath temperature is

65℃ and current density is 10 A/dm2. Karthikeyan et al. [22] studied on the formation, characteristics and properties of electroless nickel phosphorous (Ni–P) coatings and electroless nickel alumina (Ni–P–Al2O3) coating with varying reducing agent concentration. The results obtained indicate that the deposition rate and surface roughness of both Ni–P coating and Ni–P–Al2O3coatings are highly influenced by reducing agent (sodium hypophosphite). The specific wear rate of Ni–P–Al2O3coated and post coating heat treated specimens was observed to be less when compared with that obtained in the case of conventional Ni–P coating. Prasanta Sahoo et al. [19] worked on the optimization of coating parameters on the tribological behaviour of Ni-P-Al2O3 coatings. They found high hardness, good wear resistance and corrosion resistance for the optimized coating parameters. It is confirmed that the wear resistance of co-deposited layer of Ni-SiC increases with increasing submicron-size vol. %SiC. The bath was stirred by a magnetic stirrer with stirring rate of 250 rpm and heated to 50^0C [23].

Wu et al. [12] **e**lectrodeposited Co-Ni-Al_2O_3 composite coatings and found that the coefficient of thermal expansion and the thermal conductivity of Co-Ni-Al_2O_3 composite coatings are varied with the increase of Co contents and the temperature. Using an optical microscope, the mean size of the α-Al_2O_3 particles was estimated to be 0.5 μm. The Al_2O_3 particles were pretreated with acetone and warm 5% HNO_3 to remove residual organic and impurities, then washed with distilled water and dried. Similar work was carried out by Srivastava et al. [24] using SiC, Si_3N_4 and Al_2O_3 particles on the structure and properties of electrodeposited Ni. The Ni based composites were electro deposited using a sulphamate electrolyte comprising of nickel sulphamate 275g/l, nickel chloride 6g/l, boric acid 30g/l and sodium lauryl sulphate 0.2g/l. The PH of the electrolyte was maintained at 4 by the addition of sulphamic acid. Ghanbari et al. [25] **e**lectro deposited Ni-Al composite coatings on the aluminum 7022 substrate. Specimens were abraded by using 1200 Sic water proof paper. After preparation samples, were dipped in zincate bath containing 30g/l Ni $(SO_4)_2$, 40g/l $ZnSO_4$, 106g/l NaOH, 10g/l KCN, 40g/l $KHC_4H_4O_6$, 5g/l $CuSO_4$, and 2g/l $FeCl_2$ for 3 min at 38^0C.The modified zincate solution is quite operative to form thin and uniform, which results from various additional elements. Chang et al. [18] fabricated Ni-Co/nano-Al_2O_3 (Ni-Co/ Al_2O_3) composite coatings were prepared under pulse reversal current (PRC) and direct current (dc) methods respectively, The wear loss of the composite coatings decreases with the introduction of the Al_2O_3 nanoparticles and decreases with the increasing of the Al_2O_3 content in the coatings. With the increasing of Al_2O_3 content, the hardness and wear resistance of the composite coatings enhanced. The PRC composite coatings exhibited compact surface, high hardness, better wear resistance and lower macro-residual stress compared with that of the dc composite coatings. The distribution of Al_2O_3 particles to the coating makes the hardness improve the hardness of the PRC composite coating is superior to that of the dc composite coating.

The present majorly concentrates on the fabrication of Ni-Alpha Al_2O_3 electro co-deposited -coatings on Al6061 substrate material. The adhesive strength and specific wear rate of the coating are studies. The design of experiments is carried out by central composite design method of response surface methodology technique.

2. Materials and Methods

2.1 Material

The Aluminium 6061 rectangular plate specimen to be coated cleaned to remove the impurities present on the surface. The uncoated region is cover with masking tape, it is connected to negative terminal and nickel is connected solution positive terminal of DC source. These electrodes are dipped in nickel electro plating solution and coating is done for specific period of time. Fig. 2.1 shows project methodology of the Ni-Al2O3 composite coating.

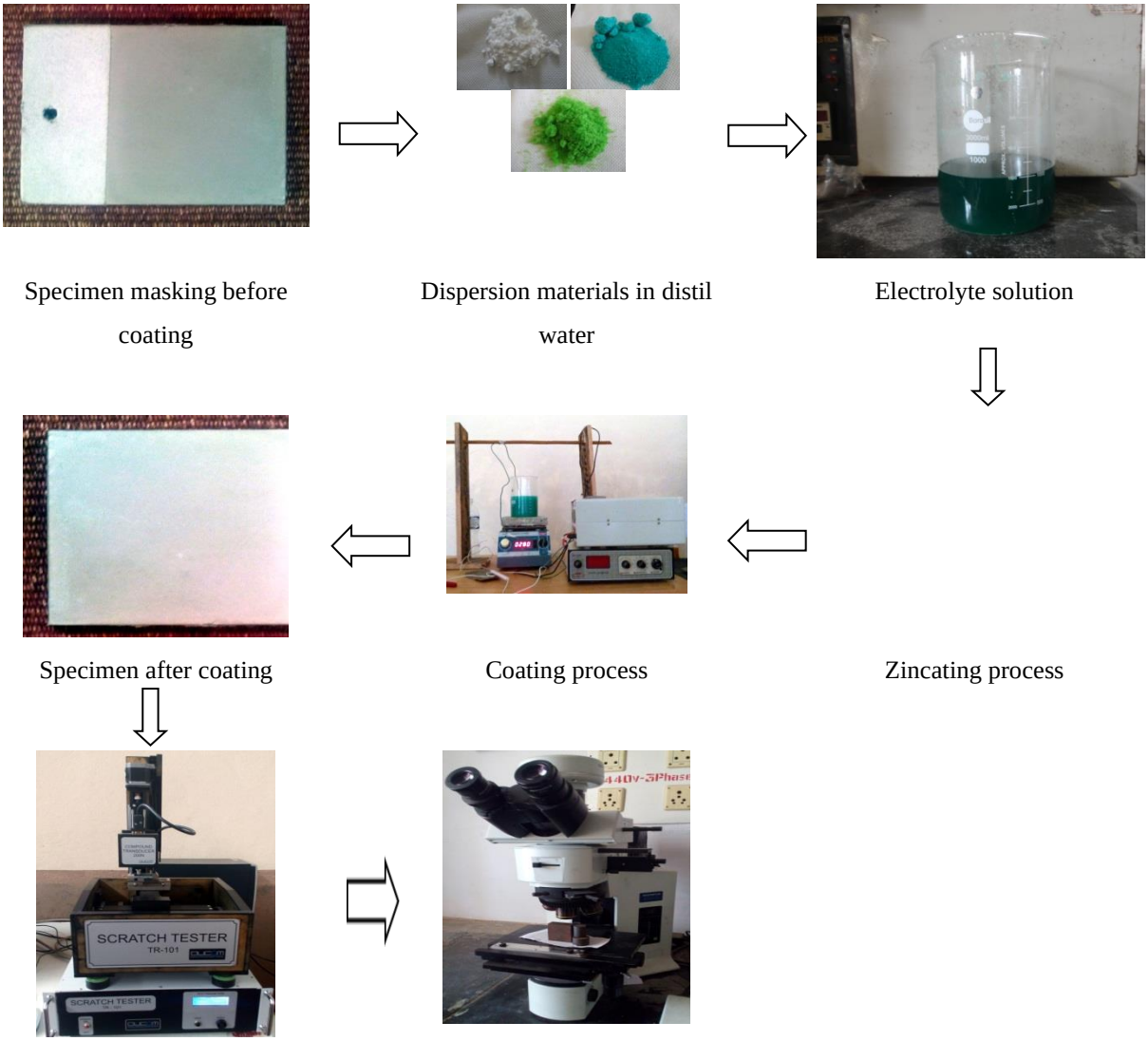

Fig. 2.1. Coating Procedure

Aluminium 6061 rectangular plate having 40×40mm is prepared based upon the American society for Testing and Materials (ASTM) standard which is to be fixed in scratch test machine. Work piece to be plated may be put through a variety of pretreating processes including surface cleaning, surface modification and washing. The motivation of pretreatment is to remove contaminants, such as dust and films from the substrate surface. The surface contamination can be extrinsic, composed of organic debris and mineral dust from the environment. The first stage was the mechanical polishing to make sure the surface to be plated is smooth and has very good surface finish. The specimen was polishing with different grits of emery papers (180,320,400,600,800 and 1000) were used.

2.2 Zincating process

Cleaning is very important step in the process of metal deposition. This process involves the use of cleaners, either with or without the application of current and frees the surface from dirt, oil, grease and so on. After mechanical polishing then next stage is the zincating process. The substrate was immersed in acetone for few minutes and kept in a NaoH stirrer for five minutes after that the substrate was washing with distilled water. Which having zincate treatment consist of 1gm $Fecl_3$ and ZnO_3 are mixed with 100ml distilled water for 45seconds and finally washing with HNO_3 20% dipping for 10 seconds. The same process will be continued. This was done to clean the sample of any impurities like oil, grease, dirt and so on are present. Then it

Vol. 21, No. 1, (2024)
ISSN: 1005-0930

was held in distilled water. Chemical and operating parameters given in the table were selected for electro-deposition of Ni-Al_2O_3 composite coating on aluminium coating (Table 4.1).

Table 4.1: Electro co-deposition plating bath composition of Ni-Al_2O_3 Composite coating.

Nickel sulphate	250g/l	
Nickel chloride	35g/l	
Boric acid	40g/l	
Al_2O_3	10g/l	
Current density, A/dm^2	2	
pH	4.0	
Temperature, °c	50	
Cathode	Nickel	
Anode	Aluminium 6061 plate	

The test specimen is Aluminium plate shown in Figure 4.1. Aluminium plate is the most common used material for the Chrome plating process. The specimen size is limited to 40mm x 60mm x 3mm and it has a 5mm hole for hanging purpose in electrolyte bath.

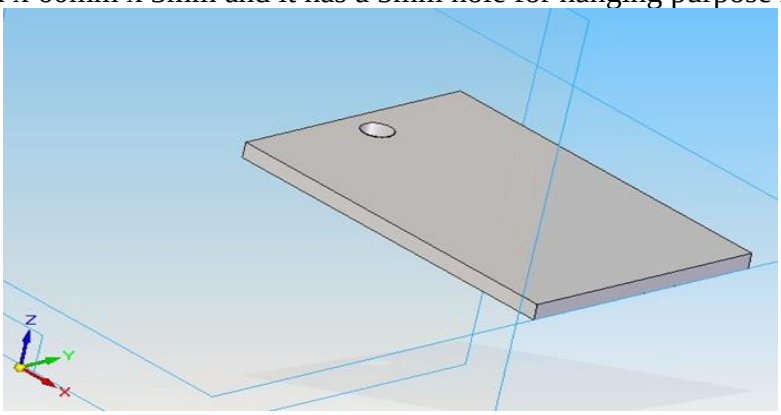

Figure 4.1 Aluminium test specimen

Samples plate is covered with 60mm masking tape on the external surface except the buffed area where the coating is finished. Pure nickel rod acts as the anode and the aluminium specimen acts as the cathode onto which desired material is coated. Both the cathode and anode

are deep into the composite electrolytic solution. The separation between the anodes is kept up between 9cm for all experiment. The electrolyte is continuously mixed with the help of magnetic stirrer at 250rpm and warmed to required temperature. Both current density and bath temperature are set to desire value. The electroplating is done for 60min. The solution is continuously stirred at regular interval to avoid the settling down of reinforcement particle. After the coating the specimen is washed in water for 10min to remove approximately adsorbed particle from the coating surface.

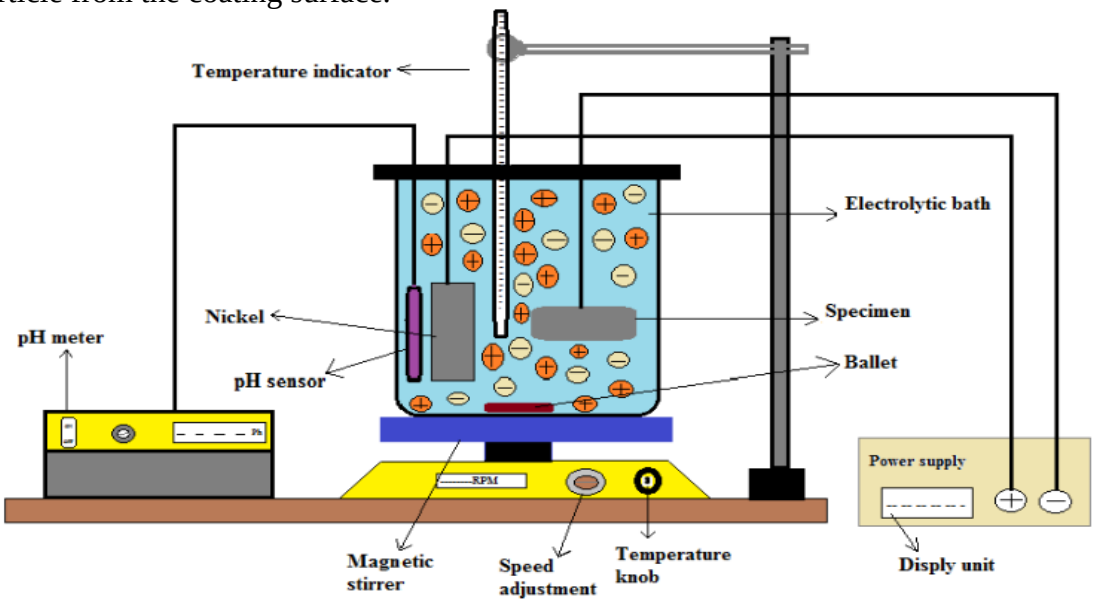

Fig.4.2 Schematic of Electrodeposition System

Scratch test is conducted by producing a scratch on the surface of the coating changing the normal load from 20 to 80 N in different stages. Scratches with progressive scar width are produced successively with a gap of 0.25mm/1.0mm in between scratches. Four different runs were conducted for each specimen and the two coinciding values are reported. Using the optical microscope Olympus which has high resolution/high contrast/clear images and scratch width images at different loads and a graphical display of forces with a sharp change in traction force indicating scratch failure were taken. Adhesion testing was performed utilizing a commercial automatic scratch analyzer (Ducom TR101, Bangalore India) equipped with a Rockwell C diamond stylus (200 μm radius). Scratches were performed by applying linearly increasing load for an interval of 10 mm. The linearly increasing load is applied from 20N to 200N at an increasing load of 10 N/mm with the horizontal speed of 0.5 mm/s. The test parameters are given in the Table 4.2.

Table 4.2. Scratch test parameters

Load type	Progressive

Vol. 21, No. 1, (2024)
ISSN: 1005-0930

Initial Lad	20N
Final load	200N
Loading rate	0-20 N/mm
Scratch Length	10 mm
Scratching speed	0.1-2.0 m/sec
Indenter geometry	120° cone
Indenter material (tip)	Diamond
Indenter tip radius	200 μm

The experimental plan with the coded and uncoded levels of design factors and experimental results are given in Table 4.5. The small, central and high levels of each factor are coded as −1, 0 and 1, correspondingly, while the lowest and highest levels are coded as -1.682 and 1.682.

Table 4.5: Experimental range of the variables studied using CCD in the terms of actual and coded factors.

Factors	Symbols		Encoded values of coded levels				
	Un Coded	Coded	-1.682	-1	0	1	1.682
Bath temp. ^{o}c	x_1	X_1	30	34	40	46	50
Current density, A/dm^2	x_2	X_2	1	1.2	1.5	1.8	2
Particle loading, gm	x_3	X_3	0	1.6	4	6.3	8

Dry sliding wear test carried out on Pin-on-disc wear test ring as per ASTM G99 standard. The schematic of the pin-on-disc wear test equipment is as shown in the fig. The disc is made of EN-32 and hardness of 64HRC is used, on which the specimen to be held firmly. ASTM G99 has given all the conditions of cleaning, preparation, load conditions, environmental conditions, safety and measurement for Pin-on-disc wear test.

The initial weights of each specimen were measured by using electronic weighing machine of least count of 0.001 gm. The fixed pin (specimen) pressed against the rotating disc when the load is applied and runs for a specified sliding distance. In the present study all the specimens of different coating parameters according to the central composite design (20 specimen) are tested on DUCOM Pin-on-disc wear test ring, under the conditions of constant load, speed and sliding distance of 20N, 1.2m/s and 1000m respectively.

3.0 Results and discussion

3.1 Scratch test

Table 3.1 shows Adhesive strength results for Ni-Al_2O_3 composite coatings.

Std order	Run order	**Factor 1** Bath temperature, °C	**Factor 2** Current density, A/dm^2	**Factor 3** Particle loading, gm	**Response** Adhesive strength, Nm/m
11	1	40	1	4	63
19	2	40	1.5	4	55
3	3	34	1.8	1.6	62
1	4	34	1.2	1.6	54
16	5	40	1.5	4	61

Vol. 21, No. 1, (2024)
ISSN: 1005-0930

18	6	40	1.5	4	45
10	7	50	1.5	4	56
4	8	46	1.8	1.6	54
20	9	40	1.5	4	56
13	10	40	1.5	0	52
8	11	46	1.8	6.3	61
7	12	34	1.8	6.3	54
17	13	40	1.5	4	62
9	14	30	1.5	4	58
6	15	46	1.2	6.3	54
15	16	40	1.5	4	51
2	17	46	1.2	1.6	63
14	18	40	1.5	8	59
12	19	40	2	4	56.08
5	20	34	1.2	6.3	57.08

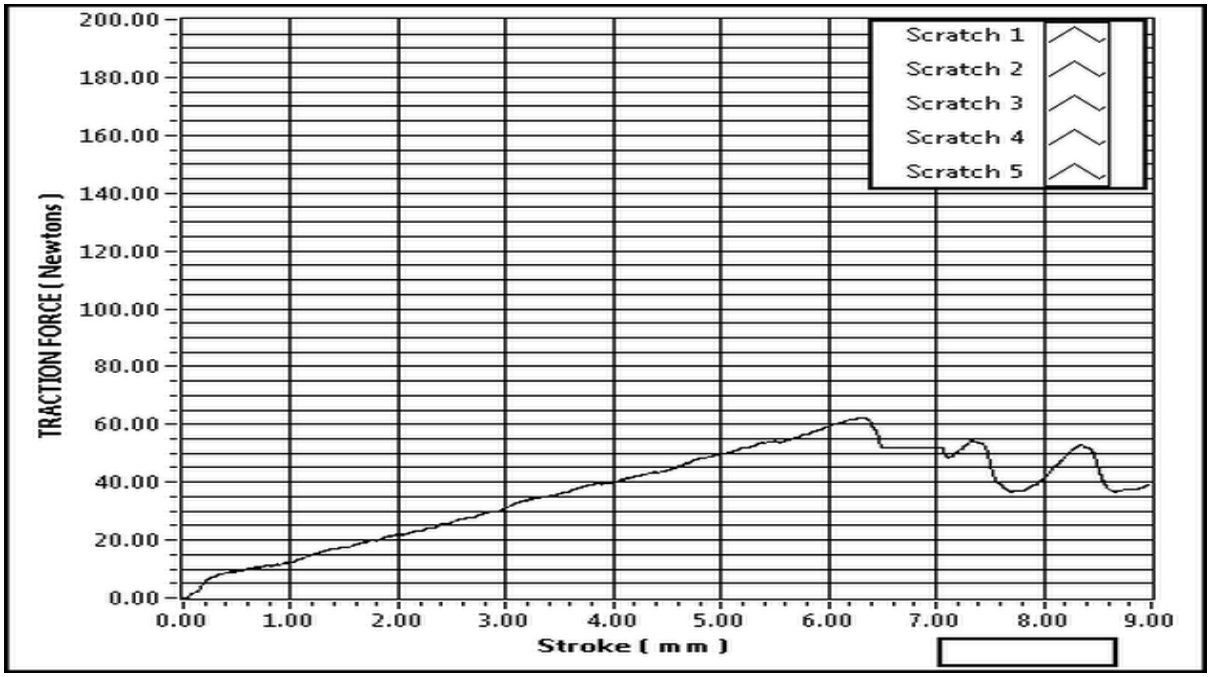

Figure 5.1 Shows the Stroke length (mm) vs. Traction force (N)

The above fig 5.1 shows the Stroke length (mm) vs. Traction force (N) under the condition Normal load: 20N, Scratch speed: 0.1mmps, Loading rate: 20npmm, Stroke Length: 9mm. The specimen used under this experiment prepared at the condition of Temp.46°C, current density 1.8A/dm^2, particle loading 6.3gm during the coating process, from the above graph. The traction force at which coating failure occurs with respect to stroke length.so traction force at which failure arises is shows at the load of 61N with respect to stroke length of 6.2mm.

Vol. 21, No. 1, (2024)
ISSN: 1005-0930

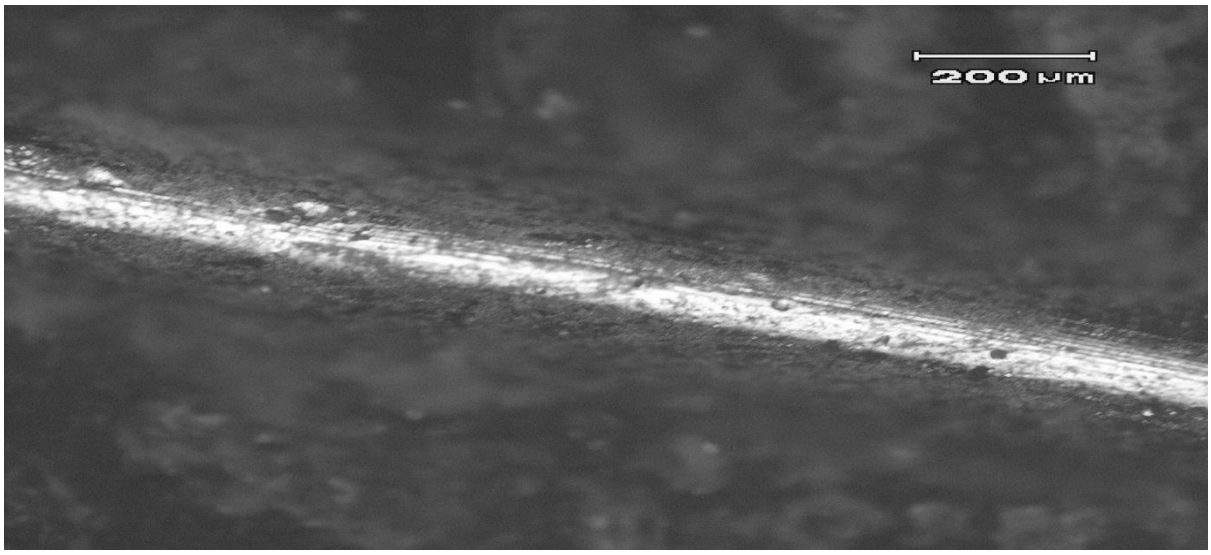

Figure 5.2 shows the Optical microscope of coating failure

The Fig. 5.2 shows the optical microscope of the scratch scar of a coating material. The main use of the optical microscope is to determine the scratch scar/track is to determine the mechanism of coating failure. Only a small number of micro cracks are visible, but no coating spallation can be observed.

Probability plotting is the graphical method for deciding for the model data conform to a hypothesized distribution based on a subjective visual examination of information. The general impression is that the residuals scatter randomly on the display, suggesting that the variance of the original observations is constant for all values of y. If the variance of the response depends on the mean level of y, then this plot will often exhibit a funnel shaped pattern. This is also suggestive of the need for transformation of the response variable y. The typical plot of residuals weight loss is shown in the figure 5.3.1 plots delights the residual are falling on the straight line, it implies error are dispersed normally.

Vol. 21, No. 1, (2024)
ISSN: 1005-0930

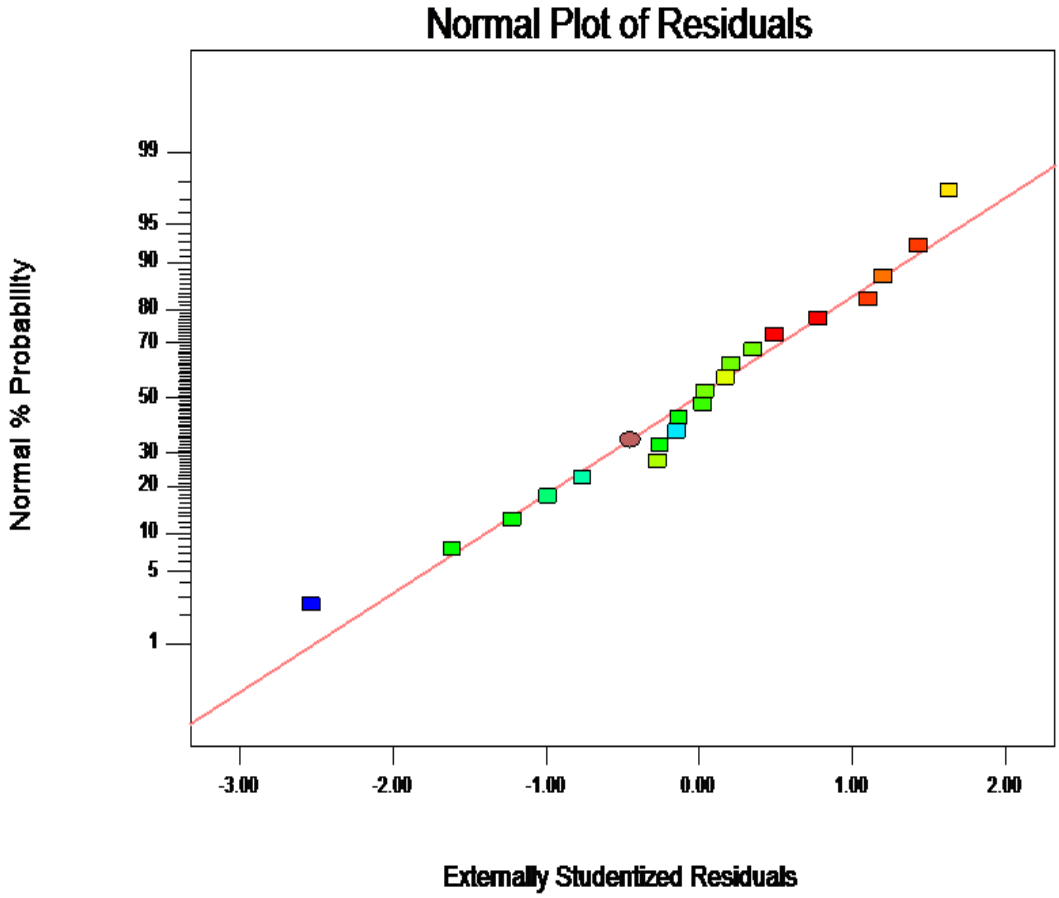

Fig.5.3.1 Normal plate for adhesive strength of composite coating material

Vol. 21, No. 1, (2024)
ISSN: 1005-0930

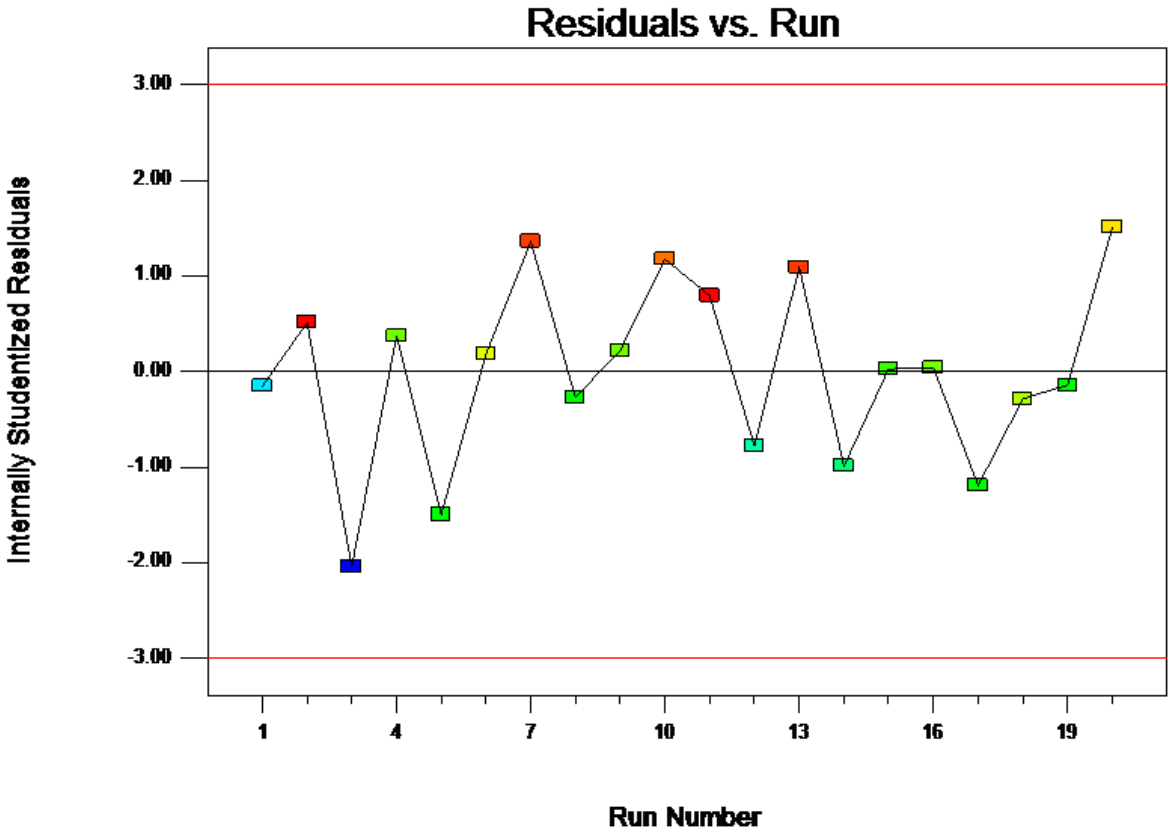

Fig. 5.3.2 Residual plot for Adhesive strength of composite coating

Figure 5.3.3 shows that predicted value are well fitted with actual value; at some point variation in the value is due to error in the experimental. The input parameters are selected randomly within the experimental domain to validate the mathematical model.

Vol. 21, No. 1, (2024)
ISSN: 1005-0930

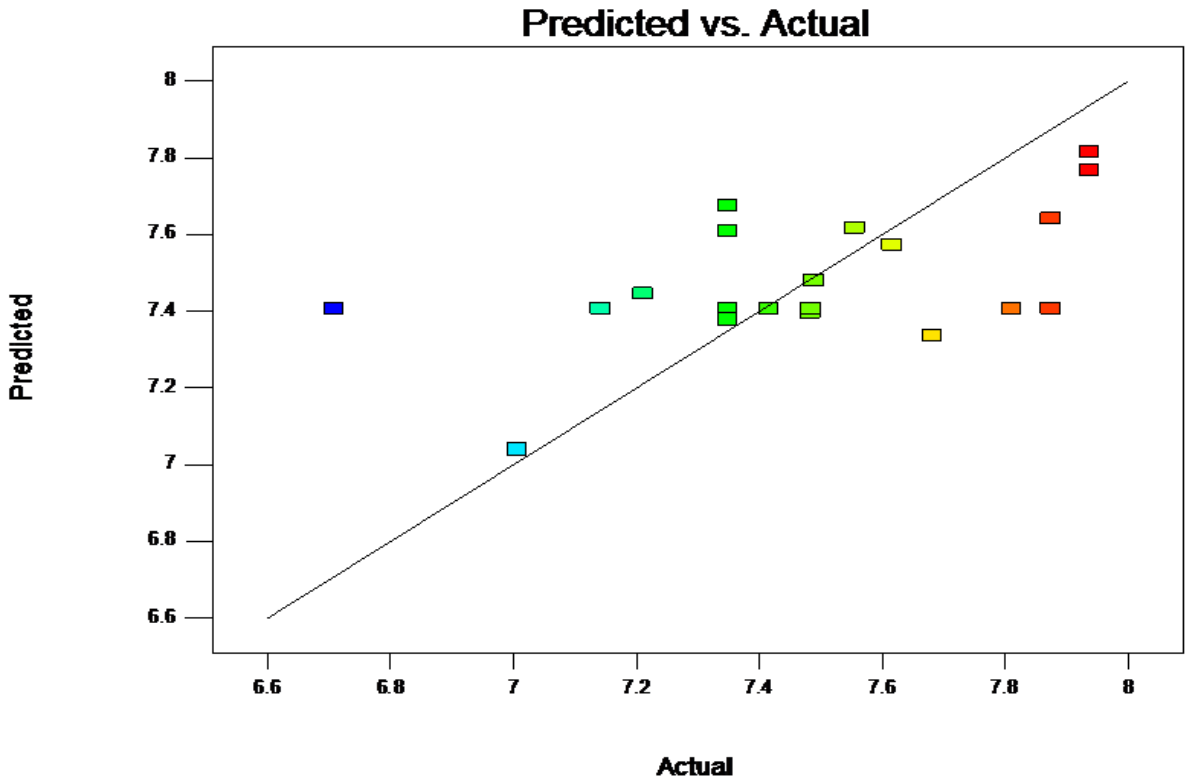

Figure 5.3.3: Actual and predicted values of composite coating

If the model is correct then the assumptions are satisfied, the residual should be structure less in specific, they should be unrelated to any other variable including the predicted response. A straightforward check is to plot the predicted value and response. This plot should not releve any boos pattern. Figure 5.3.4 shows the residual and predicted value for coated specimens.

A defect that occasionally shows up on this plot is non-constant variance. Sometime variation of the observation increases with increasing the magnitude of observation. This would be the case if the error in the experiment was a constant percentage of the size of the observation. If this were the case residual would get larger as the predicted value increases. And look like an outward opening funnel.

Vol. 21, No. 1, (2024)
ISSN: 1005-0930

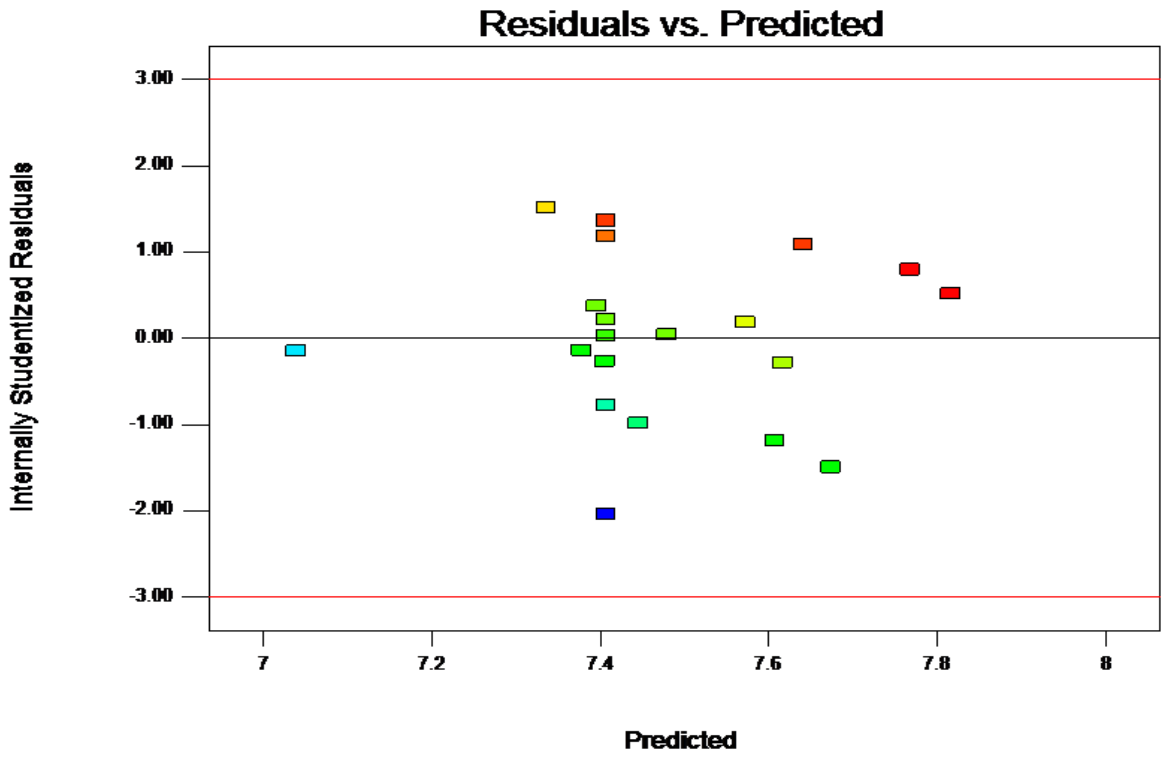

Figure 5.3.4: Residual v/s predicted value for composite coating

5.3.1 Main effect plot for Ni-Al_2O_3 composite coating

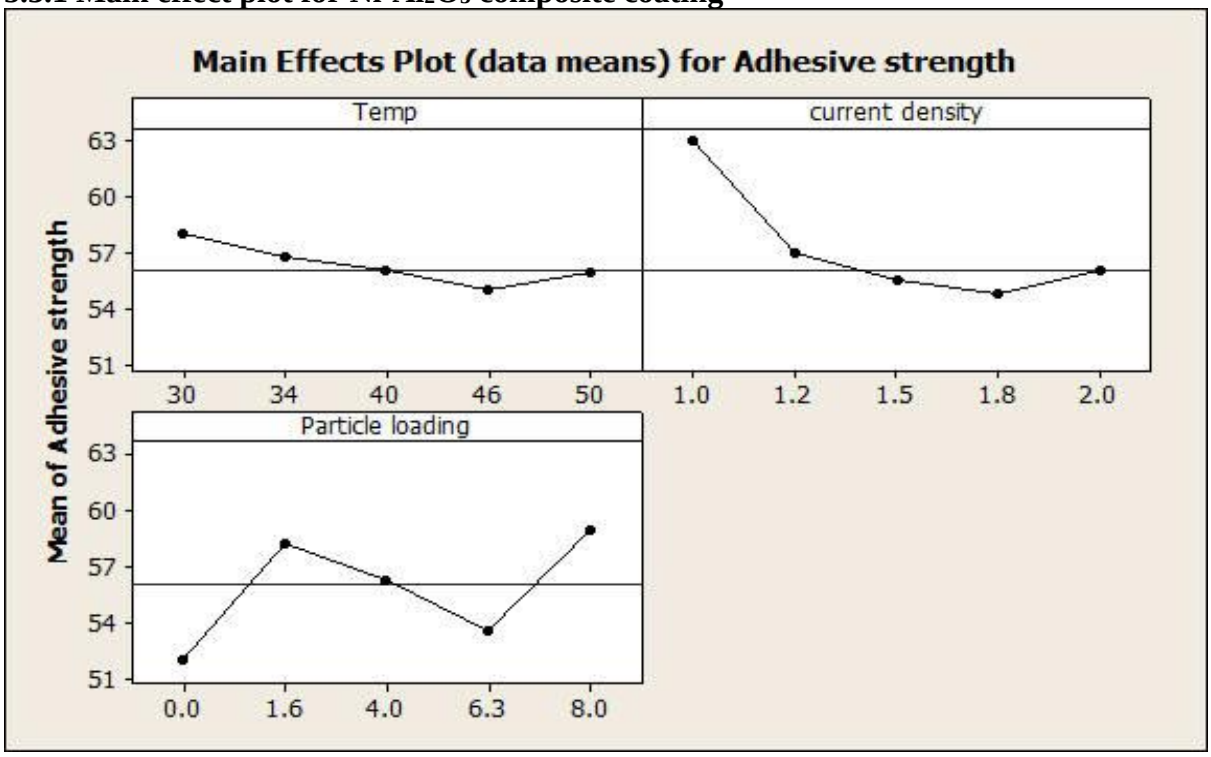

Figure 5.3.5: Main effect plot for Ni-Al_2O_3 composite coating

Vol. 21, No. 1, (2024)
ISSN: 1005-0930

Figure.5.3.5 shows graphically the main effect of control factors on the adhesive strength of the Ni-Al_2O_3 composite coating material. In this main effect there is a different level of a factor affect response differently.

A main effect plot graphs the mean response for each factor level connected by line. When line is horizontal, then there is no main effect present. Each level of the factor affects the response adhesive strength same way and response mean is the same across all factors levels. By observing the above main effects plot it is concluded that adhesive strength of Ni-Al_2O_3 composite coating is when the temperature increases with increasing then the adhesive strength of coating material will be decreases with increases at temp.50°C shown in main plot. When the current density increases with increasing then adhesive strength of the coating material is decreases with increase at current density 2A/dm^2 and when Particle loading is increases with increasing then the adhesive strength of coating material is increases with 8gm.

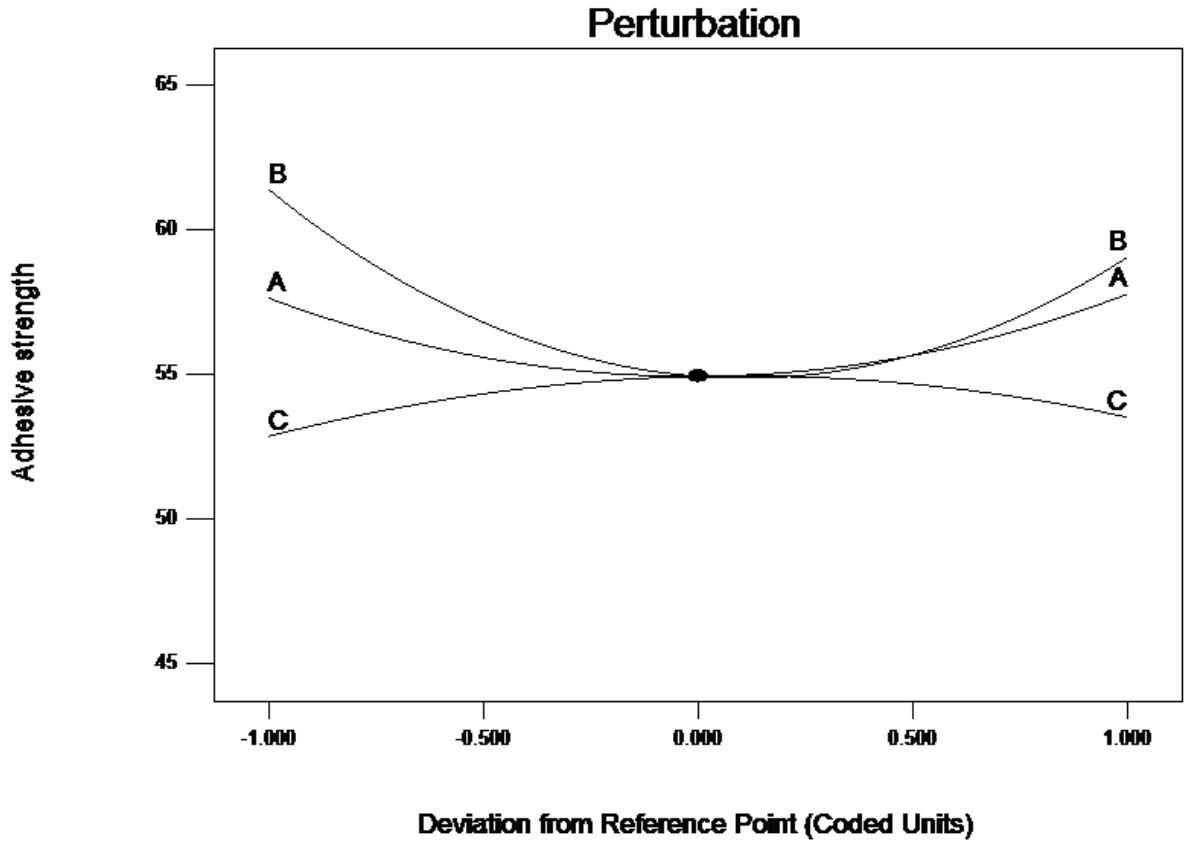

Figure 5.3.6: Perturbation plots for composite coating

To study the effect of temperature, Current density and Particle loading on the scratch behavior an empirical relationship is used. Based on this the effects of the process are graphed as perturbation plots which is as shown in figure 5.3.6. Perturbation plot represents a significant diagrammatic resprentation by providing an outline response for the data; later these responses are utilized to compare the effect of all the parameter at a point in RSM design space.

The effect of temperature, Current density and Particle loading on Adhesive strength of Ni-Al_20_3 composite coating is shown in fig. the magnitude of temp.is important since it increases the area of contact and depth undergoes large deformation.

5.3.7 Interaction plots

The effect of one factor depends on the level of the other factor we use interaction plots, the above plots temperature (A), current density (B), particle loading (C), which will interrelated with one another.

Vol. 21, No. 1, (2024)
ISSN: 1005-0930

In this graph we have to observe three types of curves middle one is slightly skewed which are interrelated with different factors and trials, adhesive strength is gradually decreases in this area. The above curve is concave shaped curve here adhesive strength is decrease at the middle point and gradually increases at the end region. The below curve slightly convex shaped, here adhesive strength is decrease at the middle point and gradually increases at the end region.

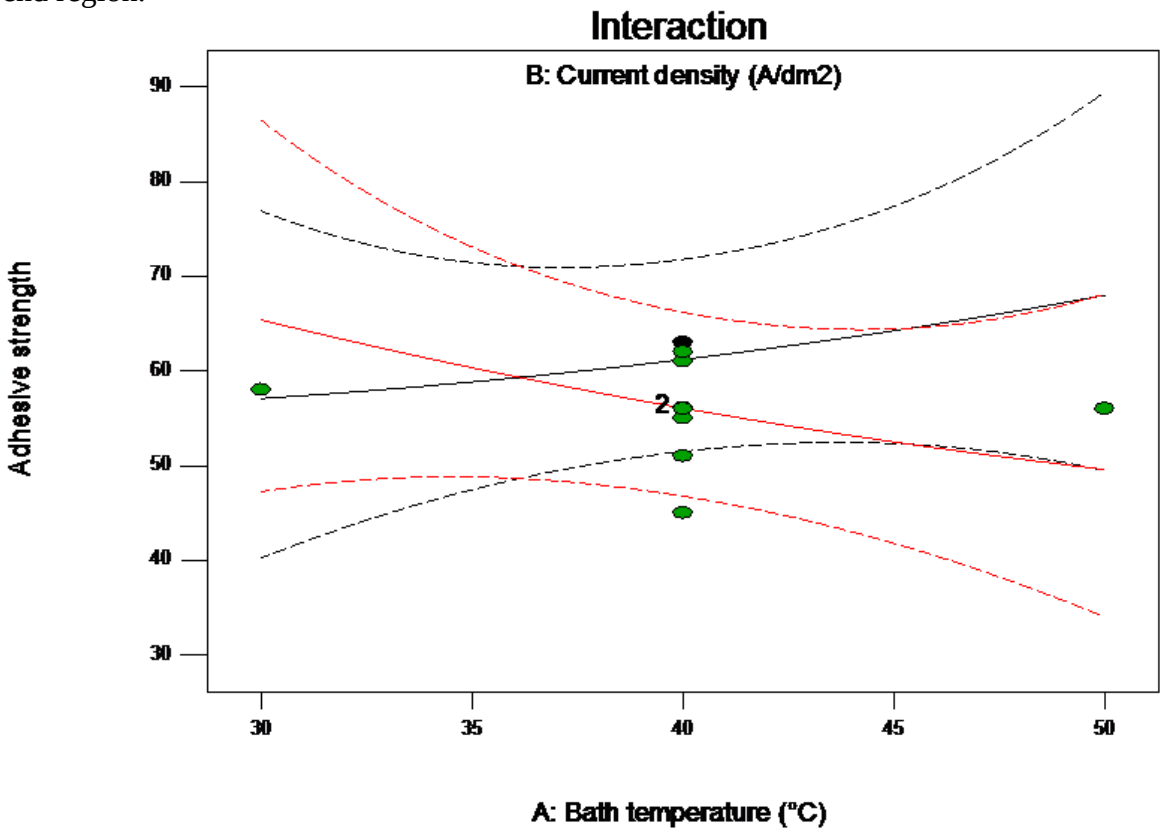

Figure 5.3.7: Interaction effects of temperature, current density, and particle loading on adhesive strength of the composite coating material

3.2 Wear results

The results are analyzed through generated plots and ANOVA to get the optimization of coating parameters.

Table 6.2 dry sliding wear results for Ni-Al_2O_3 coatings

Std Order	Run Order	T (°C)	C (A/dm^2)	P (g/L)	Wear rate (mm^3/m)
1	1	34	1.2	1.2	0.029095
14	2	40	1.5	6.0	0.025037
2	3	46	1.2	1.2	0.005451
6	4	46	1.2	4.8	0.023778
13	5	40	1.5	0.0	0.023430
11	6	40	1.0	3.0	0.022518
20	7	40	1.5	3.0	0.016850
17	8	40	1.5	3.0	0.022390
5	9	34	1.2	4.8	0.043590
9	10	30	1.5	3.0	0.007249

19	11	40	1.5	3.0	0.008621
18	12	40	1.5	3.0	0.054970
3	13	34	1.8	1.2	0.055620
16	14	40	1.5	3.0	0.001406
4	15	46	1.8	1.2	0.026760
12	16	40	2.0	3.0	0.063520
15	17	40	1.5	3.0	0.063858
10	18	50	1.5	3.0	0.036160
8	19	46	1.8	4.8	0.008697
7	20	34	1.8	4.8	0.020940

To investigate the effect of three coating parameters i.e. temperature, current density and percentage of particle loading on the dry sliding wear behaviour of composite coatings, main effect plots were plotted by using Minitab-16 software.

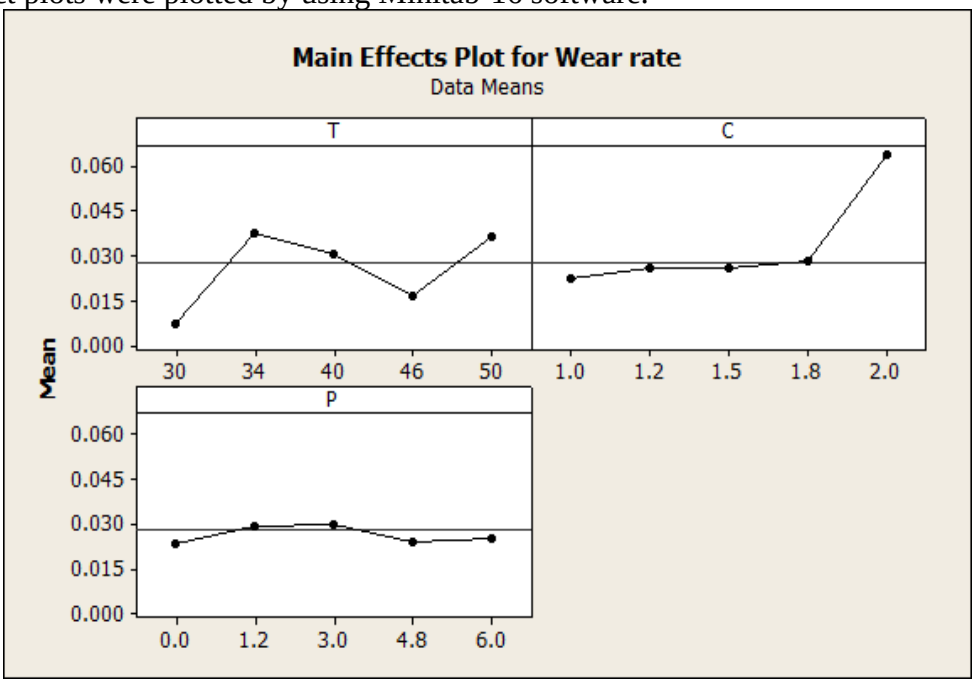

Fig. 6.2 Main effect plots of wear rate

Fig. 6.2 shows the main effect plots for wear rate, it clearly shows that the influence of temperature more followed by current density and particle loading. The plot clearly shows optimized values of these coating parameters. The optimized values are Temperature of 30^{o}C and current density of 1 A/dm^{2} and particle loading of 4.8 g/L. Interactive effects of the parameters on the wear behaviour is also plotted as interaction plots for wear which is as shown in the fig.6.3. The fig shows the interaction effect of particle loading with current density is more influencing on wear resistance.

Vol. 21, No. 1, (2024)
ISSN: 1005-0930

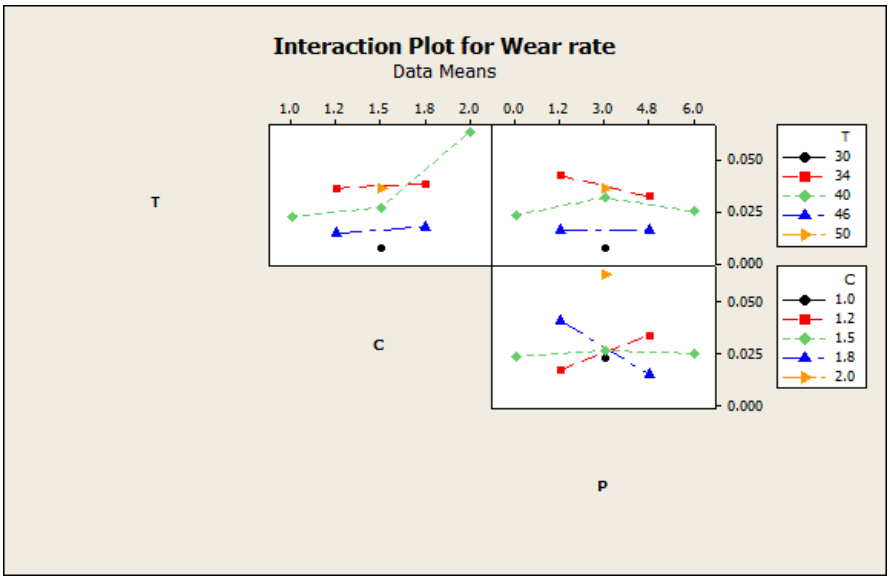

Fig. 6.3 Interaction plot of wear behaviour for respective parameters

Surface plots are generated to check the combined effect of coating parameters on dry sliding wear behavior of coatings. These plots can be used to optimize the coating parameters effectively. Fig.6.4 shows the surface plots for wear rate with respective temperature and current density. It has clearly shown that wear resistance of coatings is good at temperature of 30^{o}C and current density of 1.5 A/dm^{2}.

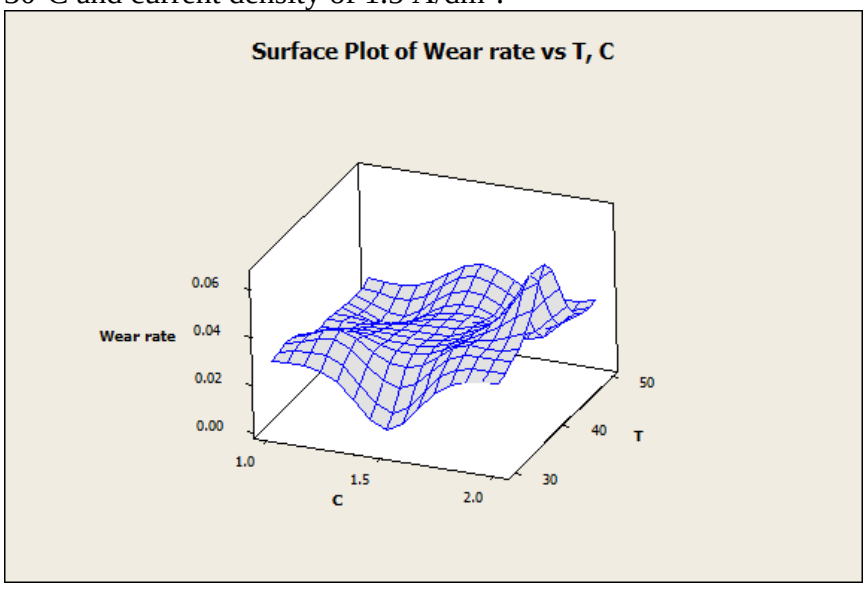

Fig. 6.4 surface plot for wear rate with respective temperature and current density

The surface plot for wear rate with respective temperature and particle loading is shown in the fig.6.5 from the plot it is clear that wear resistance is good at temperature of 46^{o}C and particle loading of 2 g/L.

Vol. 21, No. 1, (2024)
ISSN: 1005-0930

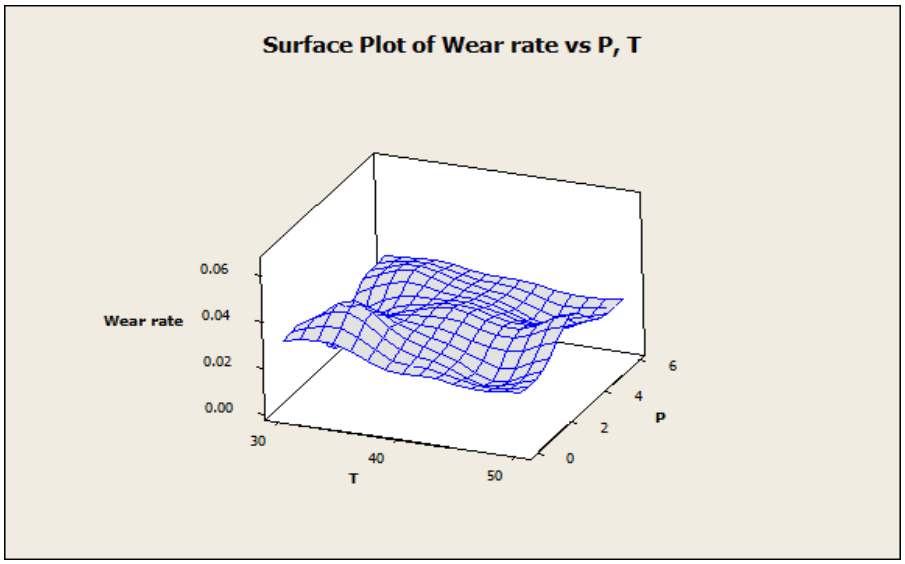

Fig. 6.5 surface plot for wear rate with respective temperature and particle loading

The surface plot for wear rates with respective current density and percentage of particle loading is shown in the fig.6.6. The plot shows that the wear resistance of coating is good at current density of 1.2 A/dm^2 and particle loading of 2 g/L.

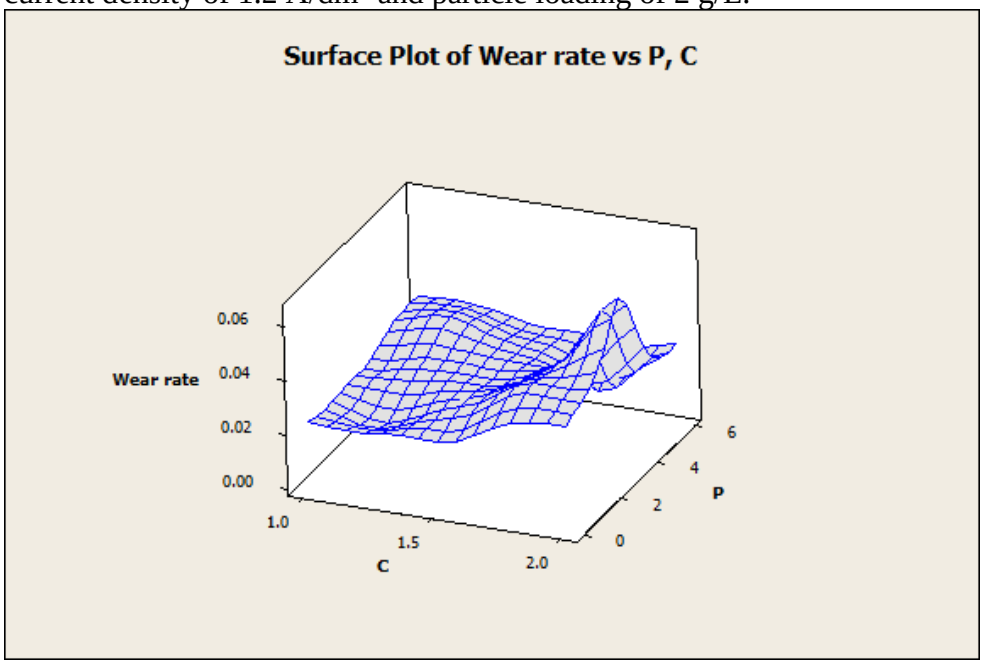

Fig. 6.6 surface plot for wear rate with respective current density and particle loading

4.0 CONCLUSION

The goal of this research work was to systematically study the effects of various process variables on the Ni-Al_2O_3 composite coating on aluminium 6061 substrate. The process variables which were studied in this work were bath temperature, current density and particle loading. Surface response method is used to analyse the electrodeposited nickel alumina composite coating and from the results of the present study, the following conclusion can be drawn.

- The image analyzer pictures of different coating deposits show that the structure is homogeneous, compact and the surface is covered by Al_2O_3 particulates.

- The traction force influenced by load, speed and hardness of the material. So traction force high at the speed of 0.1mm/sec for both constant load and ramp load condition.

- The temperature is the most influence parameter of the coating.

- The temperature and current density these parameters has a good combination of adhesive strength for constant load value 32.33N and traction force value is 61N.

- The coating replicates the profile of the substrate very closely. Traction force is influenced by the hardness of the material.

- The interaction effect of particle loading with current density is more influencing on wear resistance.
- The optimized values are temperature of 30^{o}C, current density of 1 A/dm^{2} and particle loading of 4.8 g/L.

References:

[1] J.D.M. Guerrero, B. Satpathy, P.S. Prasad, S. Das, K. Das, Electrodeposition process optimization by response surface methodologies to obtain high-corrosion resistant Zn–Ni coatings, Surf. Coatings Technol. 479 (2024) 130561. https://doi.org/10.1016/j.surfcoat.2024.130561.

[2] H. Rao, W. Li, Z. Luo, H. Liu, L. Zhu, H. Chen, Nucleation and growth mechanism of Ni/SiC composite coatings electrodeposited with micro- and nano-SiC particles, J. Mater. Res. Technol. 30 (2024) 3079–3091. https://doi.org/10.1016/j.jmrt.2024.04.008.

[3] M. Staszuk, Investigations of CrN+Cr2O3/TiO2 coatings obtained in a PVD/ALD hybrid method on austenitic 316L steel substrate, Vacuum. 207 (2023) 111653. https://doi.org/10.1016/j.vacuum.2022.111653.

[4] M. Lekka, D. Koumoulis, N. Kouloumbi, P.L. Bonora, Mechanical and anticorrosive properties of copper matrix micro- and nano-composite coatings, Electrochim. Acta. 54 (2009) 2540–2546. https://doi.org/10.1016/j.electacta.2008.04.060.

[5] Y. Wang, S.C. Tung, Scuffing and wear behavior of aluminum piston skirt coatings against aluminum cylinder bore, Wear. 225–229 (1999) 1100–1108. https://doi.org/10.1016/S0043-1648(99)00044-7.

[6] A. Góral, Nanoscale structural defects in electrodeposited Ni / Al 2 O 3 composite coatings, Surf. Coat. Technol. 319 (2017) 23–32. https://doi.org/10.1016/j.surfcoat.2017.03.061.

[7] C.R. Raghavendra, S. Basavarajappa, I. Sogalad, Sliding Wear Behaviour of Ni-α-Al 2 O 3 Nano Composite Coating at Elevated Temperatures, Colloid Interface Sci. Commun. 27 (2018) 18–25. https://doi.org/10.1016/j.colcom.2018.09.003.

[8] X. Yu, R. Jiang, Y. Gao, Y. Li, W. Gong, X. Li, W. Lü, Microstructure and wear-resistant behaviors of Al2O3-TiO2 reinforced Ni-based composite coating plasma-sprayed on 6061 aluminum alloy, Surf. Coatings Technol. 487 (2024) 131032. https://doi.org/10.1016/j.surfcoat.2024.131032.

[9] G.J.N. N. Puneeth, J. Satheesh, V. Koti, P.G. Koppad, M.R. Akbarpour, Application of Taguchi's method to study the effect of processing parameters of 4 5 Al6082/B4C/Al2SiO5 hybrid composites on mechanical properties, Mater. Res. Express. 6 (2021) 1065.

[10] M.M. Yusuf, A.B. Radwan, R.A.S. Muhammad, A. Aboubakr, Synthesis and

characterisation of Ni – B / Ni – P – CeO 2 duplex composite coatings, J. Appl. Electrochem. 0 (2018) 0. https://doi.org/10.1007/s10800-018-1168-4.
[11] N. Kumar, K. Kishore, S. Yadav, P. Sharma, Characterisation of Ni-Al2O3 composite coatings at different Al2O3 concentrations, Mater. Today Proc. (2024). https://doi.org/10.1016/j.matpr.2024.06.001.
[12] G. Wu, N. Li, D. Zhou, K. Mitsuo, Electrodeposited Co – Ni – Al 2 O 3 composite coatings, 176 (2004) 157–164. https://doi.org/10.1016/S0257-8972.
[13] R. Sarwar, B. Zulfiqar, K. Vasilios, B. Wolfgang, Water-Lubricated Ni-Based Composite (Ni – Al 2 O 3 , Ni – SiC and Ni – ZrO 2) Thin Film Coatings for Industrial Applications, Acta Metall. Sin. (English Lett. 29 (2016) 8–16. https://doi.org/10.1007/s40195-015-0354-1.
[14] P. Narasimman, M. Pushpavanam, V.M. Periasamy, Synthesis , characterization and comparison of sediment electro-codeposited nickel – micro and nano SiC composites, Appl. Surf. Sci. 258 (2011) 590–598. https://doi.org/10.1016/j.apsusc.2011.08.038.
[15] M.R. Vaezi, S.K. Sadrnezhaad, L. Nikzad, Electrodeposition of Ni – SiC nano-composite coatings and evaluation of wear and corrosion resistance and electroplating characteristics, 315 (2008) 176–182. https://doi.org/10.1016/j.colsurfa.2007.07.027.
[16] P. Narasimman, M. Pushpavanam, V.M. Periasamy, Wear and scratch resistance characteristics of electrodeposited nickel-nano and micro SiC composites, Wear. 292–293 (2012) 197–206. https://doi.org/10.1016/j.wear.2012.05.009.
[17] S. Sathish, M. Geetha, S.T. Aruna, N. Balaji, K.S. Rajam, R. Asokamani, Sliding wear behavior of plasma sprayed nanoceramic coatings for biomedical applications, Wear. 271 (2011) 934–941. https://doi.org/10.1016/j.wear.2011.03.023.
[18] L.M. Chang, M.Z. An, H.F. Guo, S.Y. Shi, Microstructure and properties of Ni – Co / nano-Al 2 O 3 composite coatings by pulse reversal current electrodeposition, 253 (2006) 2132–2137. https://doi.org/10.1016/j.apsusc.2006.04.018.
[19] P. Gadhari, P. Sahoo, Effect of process parameters on microhardness of Ni – P – Al 2 O 3 composite coatings, 6 (2014) 623–632. https://doi.org/10.1016/j.mspro.2014.07.077.
[20] O.S.I. Fayomi, A.P.I. Popoola, A. Oheiza, T. Adekeye, Microstructure , tribological and mechanical strengthening effect of multiphase Zn / ZrO 2 -SiC electrodeposited composite coatings, Int. J Ournal Adv. Manuf. Technol. 80 (2015) 1489–1495. https://doi.org/10.1007/s00170-015-7129-8.
[21] S. Yue-hai, W.E.I. Gang, X. Rong-chun, Properties and structure of RE-Ni-W-P-SiC composite coating prepared by impulse electrodeposition, (2006) 2–6.
[22] S. Karthikeyan, B. Ramamoorthy, Effect of reducing agent and nano Al2O3 particles on the properties of electroless Ni–P coating, Appl. Surf. Sci. 307 (2014) 654–660. https://doi.org/10.1016/j.apsusc.2014.04.092.
[23] K.H. Hou, M.D. Ger, L.M. Wang, S.T. Ke, The wear behaviour of electro-codeposited Ni – SiC composites, Wear. 253 (2002) 994–1003.
[24] M. Srivastava, V.K.W. Grips, K.S. Rajam, In fl uence of SiC , Si 3 N 4 and Al 2 O 3 particles on the structure and properties of electrodeposited Ni, Mater. Lett. 62 (2008) 3487–3489. https://doi.org/10.1016/j.matlet.2008.03.008.
[25] S. Ghanbari, F. Mahboubi, Corrosion resistance of electrodeposited Ni-Al composite coatings on the aluminum substrate, Mater. Des. 32 (2011) 1859–1864. https://doi.org/10.1016/j.matdes.2010.12.020.